

Design of UHF RFID Broadband Anti-metal Tag Antenna Applied on Surface of Metallic Objects

Yejun He and Zhengzheng Pan

Shenzhen Key Lab of Advanced Communications and Information Processing
College of Information Engineering, Shenzhen University, 518060, China

Email: heyejun@126.com; panzz89@126.com

<http://cie.szu.edu.cn/heyujun>

Abstract—A radio frequency identification (RFID) tag antenna mountable on metal surfaces is designed. It operates in the UHF frequency band (usually called UHF RFID tag) and is matched to the Alien Higgs-3 chip (a kind of RF IC chip). Based on the special structure of the microstrip antenna—two conducting surfaces: the antenna plane and the ground plane, we embed a pair of E-type slot to obtain broadband characteristics and use a short-circuited stub feed in the antenna plane. The antenna impedance is conveniently matched to the complex conjugate of the RF IC chip impedance so as to achieve good power transfer from the antenna to the RF IC chip. The simulation and practical measurement results show that the proposed anti-metal tag antenna structure is simple and the antenna bandwidth reaches 250 MHz when the return loss S_{11} is less than 10 dB. Also, the proposed antenna has good radiation pattern and gain.

I. INTRODUCTION

RFID (Radio Frequency Identification) is used in all areas of automatic data capture allowing contactless identification of objects using RF [1]. Due to the longer read distance, lower cost, faster read rate and many other advantages, the UHF RFID technology are receiving much attention in the world. However, the UHF RFID technology for many applications is not yet mature. The reason is largely caused by the technical problems such as the applicability of various objects and the adaptability of the different environments. In the applications of RFID [2]- [3], the tag often needs to be mounted on the surface of metal object. Since the reading distance of thin film of ordinary tags with homologous dipole antenna (one kind of UHF RFID tag) is very short on the metal surface, it can not be read due to the boundary conditions of the metal. Meanwhile, radiation frequency, input impedance and gain will be greatly affected, causing the antenna's overall performance to decline [4]- [6].

At present, some research findings are used to solve this problem. For example: (i) Develop an absorbing material [7]: the electromagnetic wave absorption material mainly relies on the characteristics of the material to absorb energy and to prevent the high-frequency reflected waves on the metal surface. In normal conditions, these high-frequency energy, when they go through the absorbing materials, has a magnetic loop resonance with the absorbing medium in the materials, and has also the eddy current losses in the loop circuit. Finally, the energy to lost in the form of heat so that the reflected

wave of the metal surfaces can be absorbed, ultimately, the return signal, which works in electronic tag cards that is in front of the absorbing materials, may greatly improve the read-write tag card sensitivity, because the return signal does not suffer from the interference of the reflected wave in the metal surfaces. But most of the high-band absorbing material cost is relatively high, so this kind of improvement method can not be widely applied in the UHF RFID tags. (ii) Increase the thickness of the medium: when the distance h of the tag away from the metal surface is 0.25 times wavelength, the reflected wave by the antenna incidents to the metal surface with the antenna radiation incident is superimposed by the same phase in the far field. The performance of the antenna at this time is greatly improved. It may also be better than the original, however, after the transformation of the antenna. The inevitable problem is that the volume of the antenna is greatly increased. It is inconvenient to be fixed on the surface of the object, so only the big measurement greatly limits the application of this transformation. (iii) Utilize specific EBG (Electromagnetic Band Gap) structures [8] because the specific EBG structures can inhibit the propagation of electromagnetic waves in a specific frequency band. By reducing the propagation of the surface wave, it improves the efficiency of the antenna, and reduces the side-lobe level to increase the gain. EBG structures can also change the phase of a reflected wave of a specific frequency band so that the antenna can be maintained a thinner thickness. But at the same time, there also exist some defects, such as the low gain and the manufacturing complexity of EBG structures.

For this purpose, we come up with a UHF anti-metal tag antenna based on the structure of the microstrip antenna and a short-circuited stub, which can be effectively applied to the metal surface recognition. Because the structure of the microstrip antenna requires a ground plane, so the metal surface can be used as its ground plane, and thus can be used to meet the design of the anti-metal tag antenna [9]- [10].

The remainder of this paper is organized as follows: Section II mainly introduces the process of tag antenna design, including the impedance matching, the antenna structure and simulation analysis. The simulation and measurement results are proposed in Section III. Section IV is the conclusion.

II. TAG ANALYSIS

A. The working principle of the tag

The working principle of the tag is shown in Fig. 1. Usually, the tag consists of a tag antenna and a tag chip (i.e. RF IC chip). Tag antenna receives RF signals transmitted by the reader and supplies the energy to the tag chip. When the energy is sufficient, the tag chip will be activated and then completes the appropriate actions according to the reader's query commands, and reflects the tag information stored on the chip to the reader by the method of backscatter modulation. Each tag has a unique electronic code, used for the identification of the mounted object. Tags are capable of storing the related data information of the objects, generally about 1K bits. In the management system of RFID, each tag corresponds to the attribute, status, number and other information of an object.

B. Impedance matching of the tag

To reduce the cost of the UHF RFID tag, we can directly connect the tag chip to the tag antenna. The equivalent circuit is shown in Fig. 2. V_a is the equivalent power source which is generated in the tag antenna when receiving electromagnetic waves. $Z_a = R_a + jX_a$ is the complex impedance of the antenna, and $Z_b = R_b + jX_b$ is the complex impedance of the chip. The Thevenin equivalent circuit shows that when the load impedance is equal to the the complex conjugate of source impedance, that is, under the "matching conditions", the output of power by the given voltage source to the load reaches maximum. So, the best matching condition of the equivalent circuit which consists of the tag antenna and the tag chip, is $Z_a = Z_b^*$, that is,

$$R_a = R_b, \quad (1)$$

$$X_a = -X_b, \quad (2)$$

In this paper, we select a Higgs-3 tag chip made by Alien Technology Co. to optimize the tag antenna, and the equivalent circuit of the Higgs-3 chip [11] is shown in Fig. 3. It consists of a resistance of 1500 Ω and a capacitance of 0.85 pF in parallel, and then in series with a voltage source with an internal resistance of 50 Ω . Using ADS software, we simulate the equivalent circuit to get the available impedance of the chip in different frequency as shown in Fig. 4, where Fig. 4(a) and Fig. 4(b) show the real part and the imaginary part of the matching value with different frequencies, respectively.

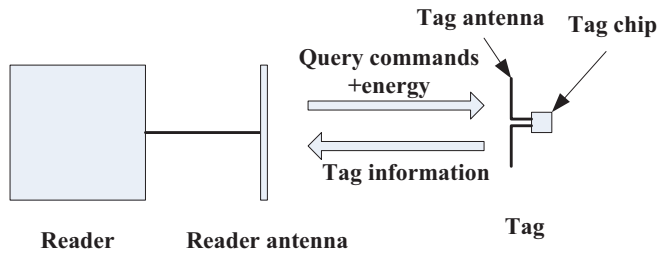


Fig. 1. The working principle of the tag.

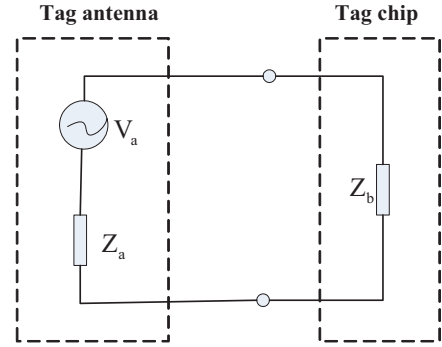


Fig. 2. Equivalent circuit of the UHF RFID tag.

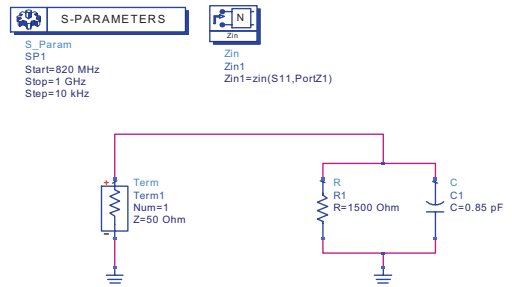
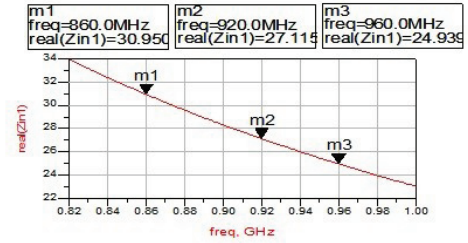
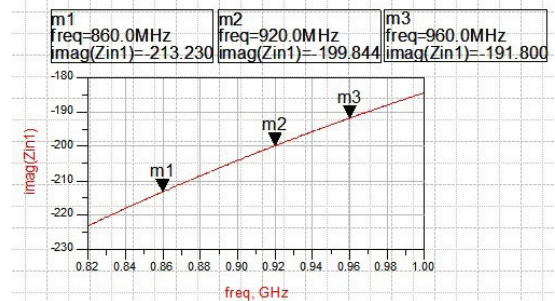


Fig. 3. Equivalent circuit of the Higgs-3 chip.



(a)



(b)

Fig. 4. Impedance of the Higgs-3 chip with different frequency. (a) Real part. (b) Imaginary part.

III. TAG ANTENNA DESIGN

A. Size of the radiation patch estimation

The first step to set the microstrip antenna is to choose a suitable dielectric substrate. If the dielectric constant is ϵ_r , the thickness of the substrate is h . For a rectangular microstrip antenna whose operating frequency is f , we could use the formula to design the efficient radiation patch width of w ,

$$w = \frac{c}{2f} \left(\frac{\epsilon_r + 1}{2} \right)^{-\frac{1}{2}} \quad (3)$$

where c is speed of light. The length of radiation patch generally takes $\lambda_e/2$, and the λ_e is the wavelength of guided wave in medium as follows,

$$\lambda_e = \frac{c}{f\sqrt{\epsilon_e}} \quad (4)$$

Considering the edge effects of shortening, in fact, the radiation unit length L should be:

$$L = \frac{c}{f\sqrt{\epsilon_e}} - 2\Delta L \quad (5)$$

where ϵ_e is the effective dielectric constant, ΔL is the equivalent radiation gap length, which are given by

$$\epsilon_e = \frac{\epsilon_r + 1}{2} + \frac{\epsilon_r - 1}{2} \left(1 + 12 \frac{h}{w} \right)^{-\frac{1}{2}} \quad (6)$$

$$\Delta L = 0.412h \frac{(\epsilon_e + 0.3)(w/h + 0.264)}{(\epsilon_e - 0.258)(w/h + 0.8)} \quad (7)$$

B. The proposed tag antenna structure

The proposed tag antenna structure is shown in Fig. 5. It mainly consists of a radiating antenna, a short-circuited stub, a ground plane and a shorting via. The antenna is made of a FR4 with double-sided metal. The thickness of the dielectric slab with FR4 is 2 mm, and the relative permittivity of the dielectric is 4.6. The top view plot is the antenna radiation plane (the length is L_1 , and the width is W_1), the bottom view plot is the ground plane (the length is L_1 , and the width is W_1). In order to reduce the size of the antenna and the input impedance, we use the embedded structure—short-circuited feed [12], the embedded depth is L_{in} , and the embedded width is W_{in} . The antenna radiating surface with a short-circuited stub is mounted to a RF IC chip. A radiation pin of the chip is connected to the antenna radiating surface and a ground pin to the short-circuited stub whose other end is connected to the metal ground plane through metal via. Here, the short-circuit stub length is L_s , and its width is W_s . One pair of E-shaped slot are embedded in the antenna radiating surface which are parallel and symmetrical with regard to the y -axis. Due to the E-shaped slot, there will be a new resonance point. By adjusting the E-shaped slot size, the two resonant points will move closer to each other and get the broadband characteristics [13]- [15]. The size of the antenna radiation patch can be calculated by equations (3)-(7), and they are shown in Fig. 5 ($L_1=75$ mm, $W_1=42$ mm, $W_s=3$ mm, $W_{in}=10$ mm). L_{in} , L_s , W_e , L_e and W_d need to be further evaluated so that

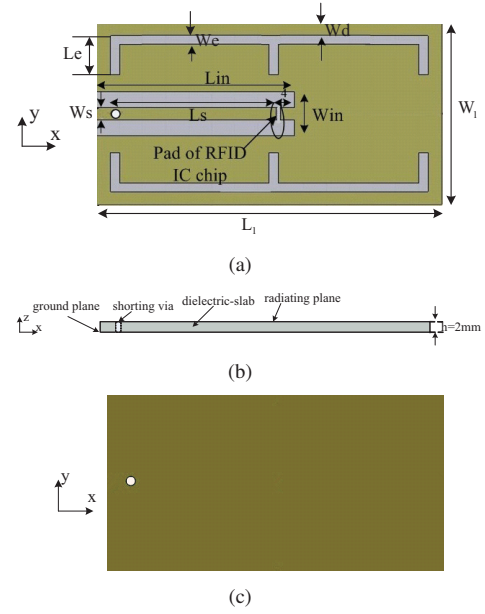


Fig. 5. The proposed tag antenna structure. (a) Top view. (b) Side view. (c) Bottom view.

the antenna can achieve impedance matching and broadband characteristics.

C. Simulation Analysis

The proposed tag antenna is simulated by HFSS software, where we set the center frequency to 920 MHz, a frequency sweep ranging from 720 MHz to 1120 MHz and the step size of 5 MHz. In order to simulate the true parameters of the tag antenna on the metal surface, the simulation of the tag antenna is mounted to the reference metal plane whose size is 100×70 mm². The radiating antenna, the ground plane, the shorting via and short-circuited stub are finite conductivity boundary as shown in Fig. 6.

From Fig. 4, we can see that when the center frequency is 920 MHz, the needed impedance should be $(27.115 + j199.844) \Omega$ to achieve impedance matching. And then, we take an example to analyze the impedance adjustment by using

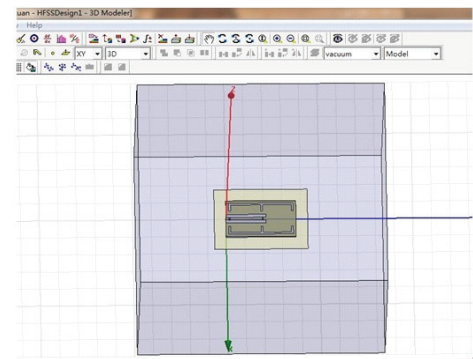
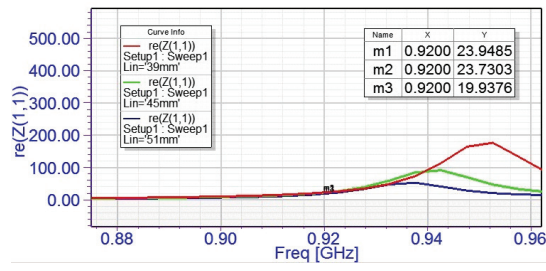
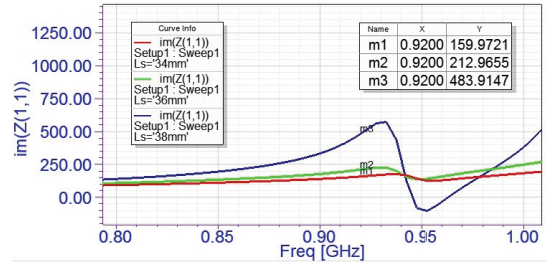


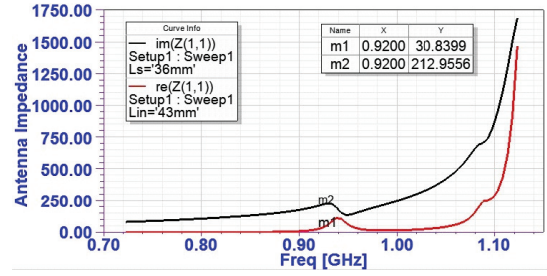
Fig. 6. HFSS modeling map.



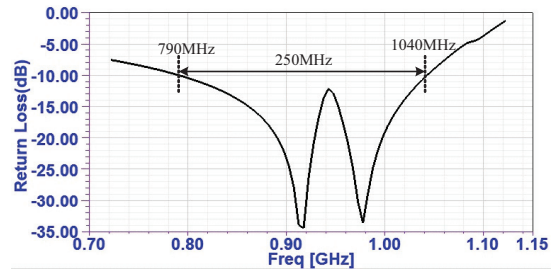
(a)



(b)



(a)



(b)

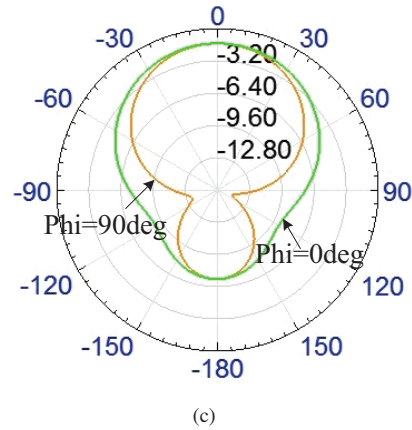
Fig. 7. Impedance control analysis. (a) The resistance of the antenna with different Lin . (b) The reactance of the antenna with different Ls .

the parameters Lin and Ls . The embedded depth Lin mainly adjusts the real part of input impedance and the short-circuited stub length Ls mainly regulates the imaginary part of the input impedance of the antenna. Simulation diagram is shown in Fig. 7.

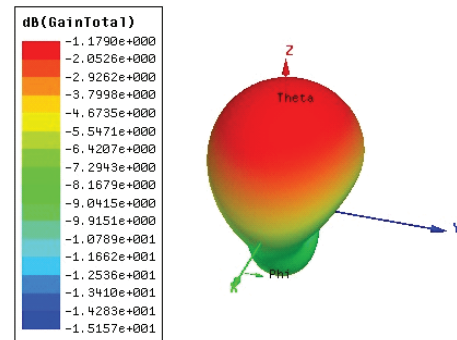
Near 920 MHz, we can see in Fig. 7(a) that increasing the embedding depth Lin can reduce the resistance of the input impedance of the antenna. We can see from Fig. 7(b) that increasing the short-circuited stub length Ls can increase the reactance of the input impedance. Similarly, we can analyze the influence of the impedance under resonance model when changing We , Le and Wd .

Further simulation finally determines our model parameters of $Lin = 43$ mm, $Ls=36$ mm, $We=2$ mm, $Le=9$ mm, $Wd=3$ mm. By using these parameters, simulation results are shown in Fig. 8.

Fig 8(a) is the impedance matching curve. At 920 MHz, the imaginary part of the matching value is 212.9556 Ω , the real part is 30.8399 Ω . Although there are some differences with the theoretical values, the difference values are within the allowable range. Fig 8(b) is the return loss S_{11} curve, and the bandwidth reaches 250 MHz when S_{11} is less than 10 dB. It has obvious broadband characteristics. From the radiation pattern shown in Fig 8(c), we can find that the lower semi-circle is far less than upper semi-circle. So it complies with the radiation requirements of the anti-metal tag antenna. Fig 8(d) is the three-dimensional radiation pattern at 920 MHz.



(c)



(d)

Fig. 8. Simulation results. (a) Impedance matching curve. (b) Return loss S_{11} curve. (c) Two-dimensional radiation pattern when $\Phi=90^\circ$ (YOZ plane) and $\Phi=0^\circ$ (XOZ plane). (d) Three-dimensional radiation pattern at 920 MHz.

IV. MEASUREMENT RESULTS

According to the size of the tag antenna designed above, the anti-metal tag antenna made is shown in Fig. 9.

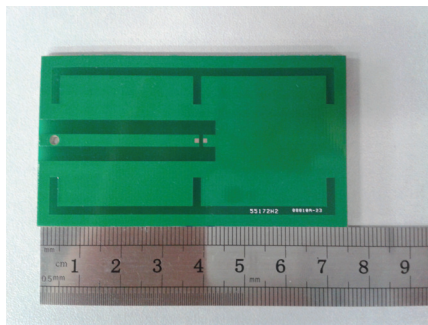


Fig. 9. Physical map of anti-metal tag antenna.

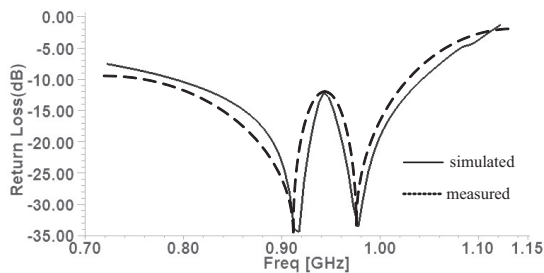


Fig. 10. Simulated and measured return loss.

Tag antenna whose size is 75 mm×42 mm is put on the metal plane whose size is 100 mm×70 mm. The reason is that we have used the reference metal plane size of 100 mm×70 mm when the antenna is simulated. We use the Alien Higgs-3 chip supported by the ISO 18000 standard. We also use the 7527 handset produced by the Psion Teklogix to test it. When the center frequency is 920 MHz, the reading distance is more than 2 m, which meets the requirements of the general application of the tag antenna. The antenna is measured by Agilent's E5071C network analyzer. Although the factors such as material processing, the simulated results and measured results have minor differences as shown in Fig. 10, the performance is still good. In the dark room conditions, the gain is measured as shown in Fig. 11 (TO_H and TO_V mean H-plane and E-plane, respectively). At 920 MHz, the gain comparison between the simulation value and the measured value is shown in Table I. The main reason why there are some gaps between them is as follows, Firstly, in the measurement process, the tag antenna and the measuring instruments need to be connected by a transmission line. According to the characteristics of the transmission line, signals may have some loss in this part of transmission lines. Secondly, the error comes from the measurement environment. Under practical conditions, the ideal dark room does not exist, so the absorbing materials of the dark room will produce reflection. Thirdly, there are some errors caused by the experimental equipments in the whole measurement system.

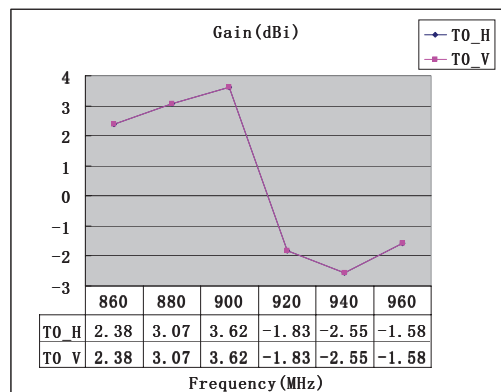


Fig. 11. Measured gain

TABLE I
COMPARISON OF THE GAIN AT 920MHZ

	Gain (dBi)
Simulated	-1.18
Measured	-1.83

V. CONCLUSION

In this paper we designed a broadband anti-metal tag antenna near the center frequency of 920 MHz. Taking the impedance adjustment and the size into consideration, we use short-circuited stub to feed and regulate impedance match effectively by regulating the embedded depth of E-shaped slot and the length of the short-circuited stub. The simulation results show that E-shaped slot design is effective in achieving the broadband characteristics. When the proposed tag antenna is mounted on the surface of metal objects, the impedance has certain stability to meet the requirements for applications.

ACKNOWLEDGMENT

This work was supported in part by The National Natural Science Foundation of China (No. 60972037), The Fundamental Research Program of Shenzhen City (No. JC201005250067A and No. JCYJ20120817163755061) and International Cooperative Program of Shenzhen City (No. ZYA201106090040A).

REFERENCES

- [1] K. Finkeneller, *RFID Handbook (3 edition)*. New York: Wiley, 2010.
- [2] J. D. Kraus and R. J. Marhefka, *Antennas: For all applications*. New York: McGraw-Hill, 2003.
- [3] Y. Liu and Q. Guan, *RFID system testing and application practice*. (in Chinese). Beijing: Publishing House of Electronics Industry, 2010.
- [4] H. W. Son, G. Y. Choi and C. S. Pyo, "Design of wideband RFID tag antenna for metallic surfaces," *Electronics Letters*, vol. 42, no. 5, pp. 263-265, Mar. 2006.
- [5] M. Keskilammi, L. Sydanheimo, M. Kivikoski, "Radio frequency technology for automated manufacturing and logistics control. Part 1: Passive RFID systems and the effects of antenna parameters on operational distance," *International Journal of Advanced Manufacturing Technology*, vol. 21, no. 10-11, pp. 769-774, Jul. 2003.
- [6] P. Raunonen, L. Sydanheimo and L. Ukkonen, M. Keskilammi and M. Kivikoski, "Folded dipole antenna near metal plate," *IEEE Antennas and Propagation Society International Symposium*, vol. 1, pp. 848-851, June 2003.

- [7] Xinwei Wang and Yinghua Lu, "Studies on characteristics of absorbing materials," in *Proc. International Symposium on Electromagnetic Compatibility*, pp. 512-514, May 1997.
- [8] L. Ukkonen, L. Sydanheimo and M. Kivikoski, "Patch antenna with EBG ground plane and two-layer substrate for passive RFID of metallic objects," in *Proc. IEEE Antennas and Propagation Society Int. Symp.*, vol. 1, pp. 93-96, Jun. 2004.
- [9] P. R. Foster and R. A. Burberry, "Antenna problems in RFID systems," in *Proc. IEE Colloquium on RFID Technology*, pp. 1/3-1/5, Oct. 1999.
- [10] L. Ukkonen, M. Schaffrath, L. Sydanheimo and M. Kivikoski, "Operability of folded microstrip patch-type tag antenna in the UHF RFID bands within 865-928 MHz," *IEEE Antennas and Wireless Propagation Letter*, vol. 5, no. 1, pp. 414-417, Dec. 2006.
- [11] Alien, *Higgs 3 EPC Class 1 Gen 2 RFID Tag IC*, Alien, 2012.
- [12] B. Lee and B. Yu, "Compact structure of UHF band RFID tag antenna mountable Oil metallic objects," *Microwave and Optical Technology Letters*, vol. 50, no. 1, pp. 232-234, Jan. 2008.
- [13] F. Yang, X. Zhang, X. Ye and Y. Rahmat-Samii, "Wide-band E-shaped patch antennas for wireless communications," *IEEE Transactions on Antennas and Propagation*, vol. 49, no. 7, pp. 1094-1100, Jul. 2001.
- [14] S. Jeon, Y. Yu and J. Choi, "Dual-band slot-coupled dipole antenna for 900 MHz and 2.45 GHz RFID tag application," *Electronics Letters*, vol. 42, no. 22, pp. 1259-1260, Oct. 2006.
- [15] K. L. Wong and W. H. Hsu, "A broad-band rectangular patch antenna with a pair of wide slits," *IEEE Transactions on Antennas and Propagation*, vol. 49, no. 9, pp. 1345-1347, Sep. 2001.